Article

Not peer-reviewed version

Preparation of High-Performance FeCoNi Thin Films by Magnetron Sputtering

Xiufang Zhong , YuZe Ge , Zelei Feng , Ke Chen , Guohui Jin , Lianze Ji *

Posted Date: 2 March 2026

doi: 10.20944/preprints202603.0032.v1

Keywords: medium entropy alloys; magnetic structure; magnetron sputtering; high frequency property

 doi:10.20944/preprints202603.0032.v1

Article

Preparation of High-Performance FeCoNi Thin Films by Magnetron Sputtering

Xiufang Zhong, YuZe Ge, Zelei Feng, Ke Chen, Guohui Jin and Lianze Ji *

Zhejiang Key Laboratory of Energy Conversion Materials for Advanced Motor, The College of Materials and Environmental Engineering, Hangzhou Dianzi University, Hangzhou 310018, China

* Correspondence: jlz@hdu.edu.cn

Abstract

This study explores the effects of sputtering pressure and power on FeCoNi high-entropy alloy films prepared by DC magnetron sputtering, focusing on microstructure, surface morphology, and static/high-frequency magnetic properties. In situ Lorentz TEM (LZ-TEM) was used to directly observe magnetic domain evolution. Results show that low sputtering pressure (1 mTorr) promotes strong FCC (111) crystallization, smooth and dense surfaces. Increasing pressure leads to amorphization, higher roughness, and degraded magnetic performance. Under optimized pressure, 100 W sputtering power yields the best crystallinity, smoothest surface, and optimal soft magnetic properties, including high remanence ratio, low coercivity, and clear ferromagnetic resonance in the 2–7.5 GHz range. The optimal parameters are confirmed as 1 mTorr and 100 W, producing uniform nanocrystalline FeCoNi films. In situ LZ-TEM reveals river-like domain walls, vortex–antivortex structures, and uniform magnetic moment precession, indicating weak domain pinning and excellent high-frequency magnetization consistency. This study provides experimental and theoretical support for the controllable fabrication of high-performance FeCoNi soft magnetic films for high-frequency devices.

Keywords: medium entropy alloys; magnetic structure; magnetron sputtering; high frequency property

1. Introduction

Driven by the rapid development of fifth-generation mobile communications (5G) [1,2], millimeter-wave radar [3], and high-density magnetic storage [4], modern electronic devices are rapidly evolving toward miniaturization, integration, and high-frequency operation [5]. As key functional layers in microwave passive devices including microsensors, filters, and circulators, magnetic thin films directly determine signal transmission efficiency and energy conversion quality [6] through their high-frequency magnetodynamic characteristics. For GHz-band applications, ideal soft magnetic thin films must satisfy multiple stringent requirements: high saturation magnetization (Ms) to break through the Snoek limit [7], high resistivity (ϱ) to suppress eddy-current loss, and low coercivity (Hc) with narrow ferromagnetic resonance linewidth (ΔH) for fast magnetic response and low signal attenuation [8]. However, conventional soft magnetic materials are increasingly facing performance bottlenecks [9]. Ferrites show high resistivity but low saturation magnetization (below 0.5 T), failing to meet high magnetic flux density demands. Permalloy (Ni80Fe20) exhibits favorable soft magnetic properties but is limited by moderate saturation magnetization (≈1.0 T) [10,11], restricting further device miniaturization. Fe–Co binary alloys achieve high Ms up to 2.4 T yet suffer from high coercivity and large magnetostriction [12,13]. To address these drawbacks, ternary Fe–Co–Ni alloys have attracted extensive attention [14]. As a representative medium-entropy alloy (MEA) [15,16], the FeCoNi system [17–19] integrates the high saturation magnetization of Fe–Co alloys and the low coercivity and superior corrosion resistance of Ni-based alloys via compositional tuning [20,21]. Recent studies demonstrate that this system can effectively reduce magnetic anisotropy via

 doi:10.20944/preprints202603.0032.v1

nanocrystalline [22] or amorphous structure design [15] while retaining excellent magnetic properties, making it a promising candidate for next-generation high-performance high-frequency soft magnetic films [23–25].

Electrodeposition is a common method for FeCoNi films due to its low cost, yet the organic additives it uses inevitably introduce non-magnetic impurities [26,27] (S, C, H, O) at grain boundaries. These impurities act as magnetic pinning centers, increasing coercivity and degrading film density. In contrast, magnetron sputtering (a physical vapor deposition, PVD, technique) enables high-purity film growth in a vacuum and is fully CMOS-compatible, making it ideal for the on-chip integration [28] of magnetic devices with semiconductor circuits. Despite existing research on sputtered FeCoNi films, most studies focus only on deposition rate or annealing effects on static magnetic properties. A systematic understanding of how key kinetic parameters—sputtering pressure and power—modulate the high-frequency magnetic response and microscopic domain evolution remains elusive [29–31]. These parameters directly dictate the energy and mean free path of deposited particles, governing crystallinity, grain size, and stress, which are critical to high-frequency loss mechanisms [32,33]. Furthermore, direct experimental evidence of high-frequency domain wall pinning/depinning, via in-situ microscopy [34], is lacking. To fill this gap, this study fabricated FeCoNi medium-entropy alloy (MEA) films via DC magnetron sputtering, systematically investigating the effects of pressure and power on microstructure, morphology, and high-frequency performance. Using in-situ Lorentz TEM, we visualized the dynamic domain evolution under an external field, establishing a direct link between microstructural pinning effects and macroscopic ferromagnetic resonance (FMR) behavior [35]. This work optimizes the fabrication process for superior high-frequency soft magnetic properties, providing a critical experimental basis for FeCoNi films in microwave integrated devices.

2. Experimental Procedure

Sample Preparation: The substrate was pretreated via reactive ion etching (RIE) under the following parameters: oxygen pressure of 20 Pa, power of 70 W, and etching duration of 25 seconds. After pretreatment, a 30 nm thick FeCoNi film was deposited using direct current magnetron sputtering.

LZ-TEM Characterisation: To observe magnetic structure evolution, FeCoNi films were deposited onto 100 nm thick SiNx layers using identical procedures. All samples were characterized by LZ-TEM characterisation. The magnetic field was applied along the Z-axis, with the in-plane field introduced by tilting the sample 10°. The perpendicular magnetic field component exerted negligible influence on magnetic structure evolution.

FMR characterisation: To obtain ferromagnetic resonance profiles, 5×5 mm^2 samples were fabricated on silicon substrates using the same deposition method. FMR spectra were obtained using the short-circuited microstrip line method. Samples were placed within a constructed cavity, with microwave signals were recorded using a vector network analyser. The in-plane magnetic field was generated by externally applied Helmholtz coils, whose magnetic field direction was parallel to the microwave propagation direction.

3. Results

3.1. Sputtering Pressure Analysis

FeCoNi films with a fixed thickness of 30 nm were deposited by precisely controlling the sputtering time. Figure 1 presents XRD patterns and atomic force microscopy (AFM) topography images of the films fabricated at sputtering pressures ranging from 1 to 15 mTorr. XRD analysis (Figure 1a) reveals a distinct (111) diffraction peak near $2\theta \approx 44°$ under low-pressure conditions, corresponding to the FCC structural characteristic and indicating a polycrystalline film. As sputtering pressure increases, peak intensity progressively diminishes and peak width broadens; at high pressures, the diffraction peak essentially vanishes. This demonstrates a significant reduction in long-

 doi:10.20944/preprints202603.0032.v1

range order and a gradual transition towards an amorphous state. The underlying mechanism is as follows: at high pressures, the molecular number density of the working gas increases. Sputtered particles undergo frequent collisions during transport, significantly shortening their mean free path. Consequently, the kinetic energy upon reaching the substrate is substantially reduced. Atoms struggle to diffuse and rearrange adequately on the surface, leading to random stacking and ultimately forming a structure with low crystallinity or even near-amorphous characteristics. AFM results (Figure 1b) show that at low pressure, the film surface exhibits high flatness and density with relatively uniform grain distribution. As sputtering pressure increases, however, film density and surface flatness gradually decrease, while surface roughness shows an upward trend. At low pressures, sputtered atoms have a longer mean free path and higher higher kinetic energy for surface migration, favoring uniform nucleation and ordered grain growth. Therefore,the film exhibits a dense structure and smooth surface. Conversely, at high pressures, particle collision and scattering effects are significantly enhanced. Insufficient deposition energy and limited atomic diffusion lead to more random nucleation and growth processes, ultimately resulting in lower film density and deteriorated surface morphology.

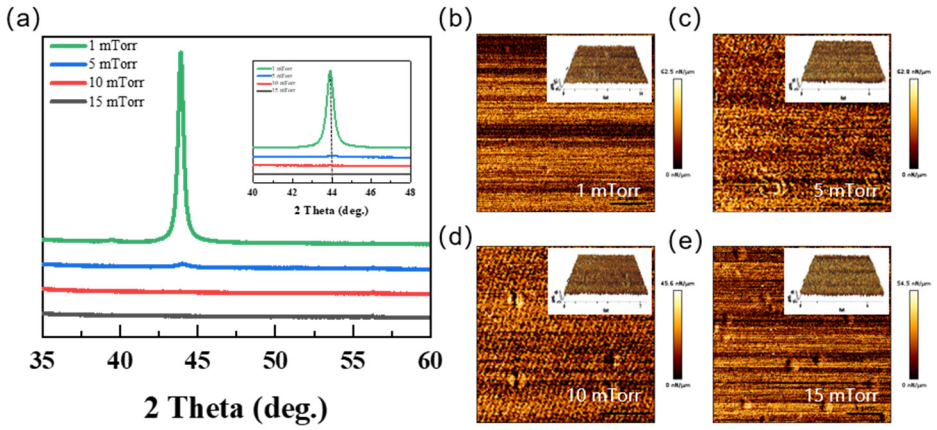

Figure 1. (a) XRD patterns of Fe-Co-Ni films grown at different sputtering pressures; (b) AFM images of Fe-Co-Ni films grown at different sputtering pressures (with the 3D image corresponding to the respective pressure displayed in the top right corner).

To investigate the effect of sputtering pressure on the static magnetic properties of thin films, room-temperature hysteresis loops were measured using SQUID. All samples exhibited similar, narrow and elongated, and approximately rectangular hysteresis loops (Figure 2a), displaying pronounced isotropic characteristics consistent with typical behaviour of soft magnetic materials. As sputtering pressure increased, the remanence of the films gradually decreased. This may stem from reduced film density and increased internal defects at elevated pressures, leading to diminished magnetic domain ordering and enhanced domain pinning effects. Consequently, magnetic moments struggle to maintain their oriented alignment removal of the external field, manifesting macroscopically as reduced remanence. Based on this, the high-frequency magnetic properties of films under varying pressures were characterised using a short-circuited microstrip line method coupled with a vector network analyser. Within the 1–5 mTorr range, the film exhibited pronounced ferromagnetic resonance behaviour (Figure 2b), with the resonance frequency progressively increasing from 2 GHz to 7.8 GHz as the applied magnetic field strengthened [36]. Conversely, no distinct resonance peaks were observed within the tested frequency range for samples at 10 mTorr and 15 mTorr high pressure. This behavior closely aligns closely with the structural evolution of the films: at elevated pressures, insufficient kinetic energy during particle deposition leads to an amorphous structure. Weakened exchange coupling reduces the effective magnetisation and

 doi:10.20944/preprints202603.0032.v1

enhances magnetic relaxation processes, ultimately weakening the high-frequency magnetic response.

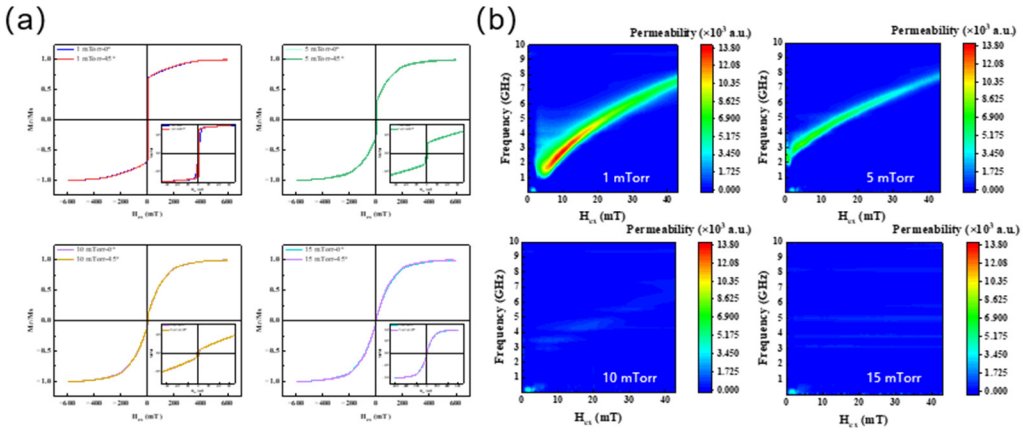

Figure 2. (a) Hysteresis loops of Fe-Co-Ni films grown under different sputtering gas pressures; (b) Ferromagnetic resonance spectra of Fe-Co-Ni films grown under different sputtering gas pressures.

3.2. Sputtering Power Analysis

Building upon optimised sputtering conditions, the influence of sputtering power (50 W–150 W) on the structure, morphology, and magnetic properties of FeCoNi thin films was further investigated. Figure 3 presents the XRD patterns and AFM topography images of continuous FeCoNi films deposited at different powers levels. All samples exhibited a broadened diffraction peak near $2\theta \approx 44°$ (Figure 3a), indicating a nanocrystalline structure. At a sputtering power of 100 W, the (111) diffraction peak intensity was highest, significantly exceeding that of the 50 W and 150 W samples. Sincethe diffraction peaks intensity directly reflects the crystallinity and grain preferential grain orientation of the film, indicating that 100 W is more conducive to the crystallisation and ordered grain growth of FeCoNi films. At low power (50 W), the lower energy of sputtered particles results in insufficient migration and diffusion capabilities of atoms on the substrate surface, hindering the formation of well-ordered grains and leading to lower crystallinity. Conversely, excessively high power (150 W) results in overly energetic particles, readily inducing strong bombardment and secondary sputtering effects on the substrate and film surface. This introduces additional defects and internal stresses, which in turn reduce crystallinity and weaken the diffraction peak intensity. Based on the earlier analysis of the influence of sputtering gas pressure on film surface morphology, we further examined the role of sputtering power. AFM results for films deposited at different power levels (Figure 3b) show that surface roughness first decreases and then increases with rising power, reaching a minimum at 100 W. At low power (50 W), insufficient particle kinetic energy limits atomic surface diffusion, resulting in lower film density and relatively pronounced micro-undulations. When power increases to 100 W, moderate particle energy facilitates more complete atomic migration and arrangement, yielding a dense, uniform film with minimal roughness. However, when power is further increased to 150 W, excessively high particle energy intensifies bombardment effects and secondary sputtering. This disrupts surface uniformity, leading to uneven grain growth and increased roughness. Therefore, an optimal power range exists for sputtering; both excessively high and low power levels degrade the surface morphology and structural uniformity of the film.

 doi:10.20944/preprints202603.0032.v1

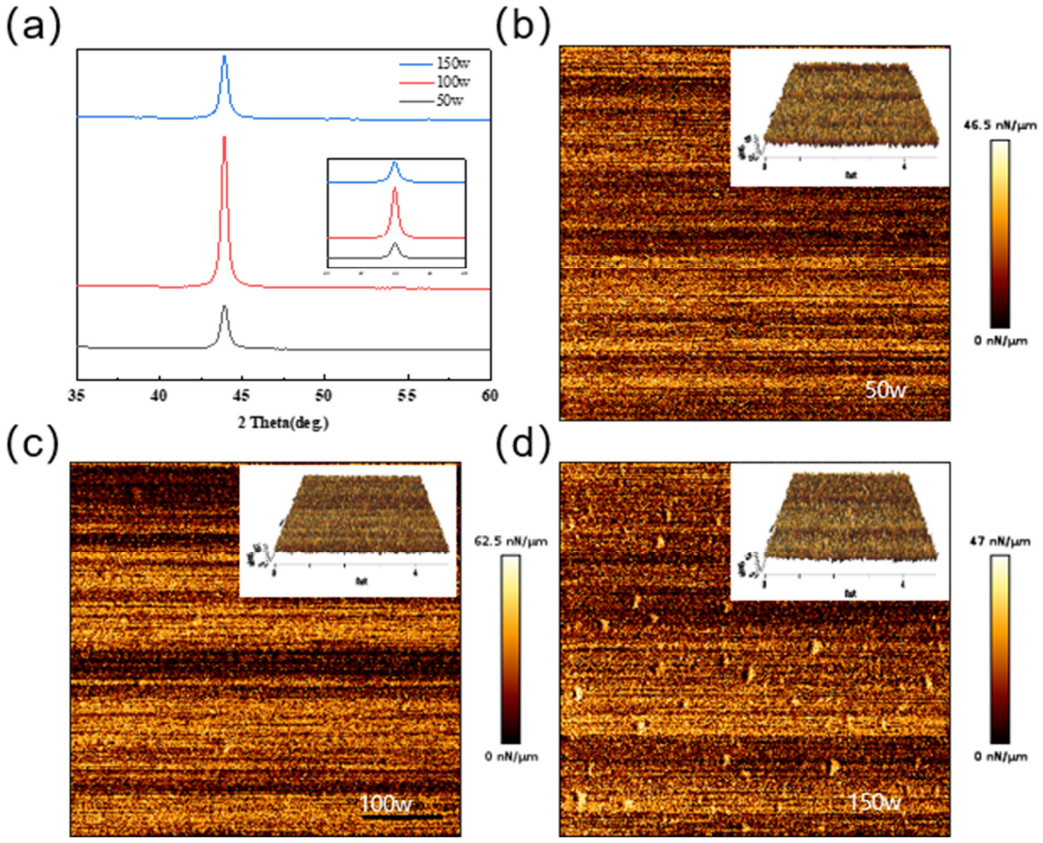

Figure 3. (a) XRD patterns of Fe-Co-Ni films grown at different sputtering powers. (b–d) AFM images of Fe-Co-Ni films grown at different sputtering powers (with corresponding 3D images at the top right corner).

Figure 4 displays the in-plane easy-axis and hard-axis normalised hysteresis loops of FeCoNi films at different power levels. All samples exhibit typical characteristics of soft magnetic materials, featuring narrow hysteresis loops and low coercivity. With increasing sputtering power, the film's remanence and remanence ratio initially rise before decreasing, reaching maximum values at 100 W and significantly outperforming samples processed at 50 W and 150 W. This trend agrees well with the XRD and AFM findings: at 100 W, the films exhibit higher crystallinity and a smoother, denser surface, facilitating uniform domain alignment and efficient magnetic moment reversal, thus yielding superior soft magnetic properties. Building upon the static magnetic characterisation, the high-frequency magnetic properties of samples fabricated at different power levels were evaluated under identical testing conditions. Figure 4b depicts the variation of the imaginary part of the film's magnetic permeability as a function of the applied magnetic field. The ferromagnetic resonance frequency of all samples shifted towards higher frequencies with increasing applied magnetic field, progressively rising from approximately 2 GHz to 7.5 GHz [37]. Notably, the 100 W sample exhibited the strongest permeability signal and the most pronounced resonance peak, directly attributable to its higher crystallinity, lower defect density, and superior microstructure.

 doi:10.20944/preprints202603.0032.v1

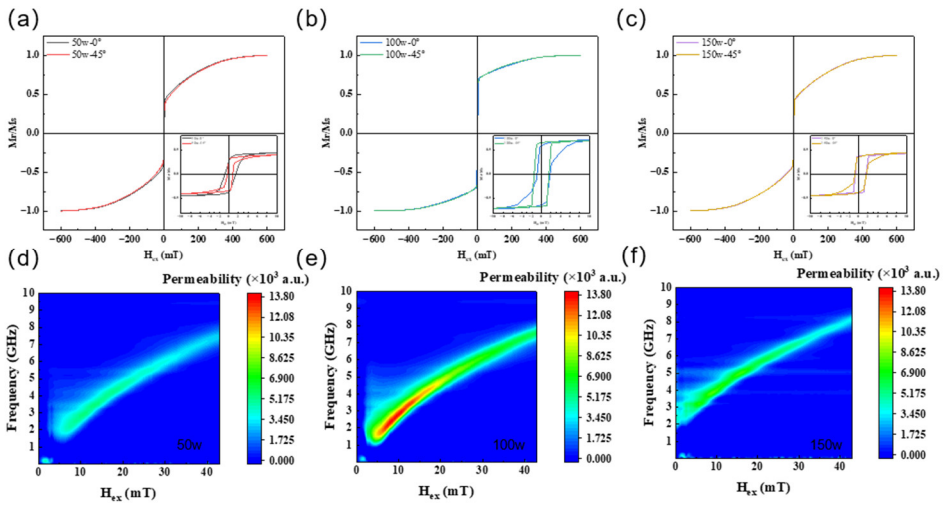

Figure 4. (a–c) Hysteresis loops of Fe-Co-Ni films grown at different sputtering powers; (d–f) Ferromagnetic resonance spectra of Fe-Co-Ni films grown at different sputtering powers.

3.3. Magnetic Domain Analysis

Integrating structural, morphological and magnetic property results, this study ultimately selected 1 mTorr and 100 W as the optimal sputtering parameters for subsequent magnetic structure characterisation. Under vacuum conditions, a 30 nm thick FeCoNi film was deposited onto a 100 nm SiNx buffer layer via direct current magnetron sputtering. Building upon this, in situ Lorentz transmission electron microscopy (LZ-TEM) was employed to visually characterise the magnetic domain structure and magnetisation dynamics of the continuous FeCoNi film. Results indicate that in the as-deposited continuous film, magnetic domain walls nucleate in a river-like domain wall configuration (Figure 5). During demagnetisation, these river-like domain walls gradually disappear; As an in-plane magnetic field was progressively applied, vortex-antivortex pairs began to emerge within the system, forming meandering domain wall structures between them. Upon further strengthening of the external magnetic field, the network structure formed by the meandering domain walls gradually disappeared. The magnetic moment orientation progressively aligned with the external field direction, ultimately reaching a saturated magnetisation state.The evolution patterns of magnetic domains reveal that within the FeCoNi continuous film fabricated under optimal conditions, the pinning forces acting on domain walls are relatively weak. Consequently, the magnetic moments can achieve coherent precession under the influence of an external magnetic field. It is precisely this low-pinning, high-coherence magnetic moment dynamics that enables the continuous film to maintain a distinct ferromagnetic resonance response under high-frequency conditions. Moreover, the resonance frequency exhibits a significant increase with rising external field strength, providing strong corroboration for the high-frequency magnetic property test results presented earlier.

 doi:10.20944/preprints202603.0032.v1

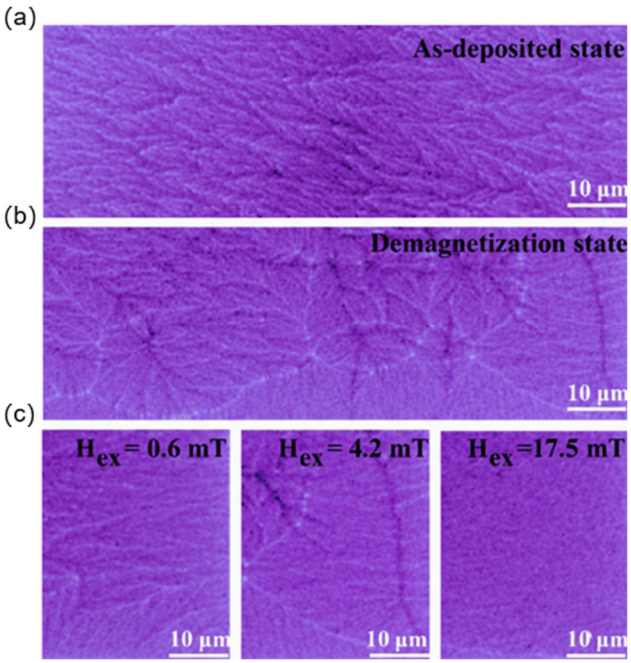

Figure 5. (a-c) Magnetic structure image of continuous film, scale bar: 10 μm, defocus amount: -6.8 mm.

4. Conclusions

This study employed direct current magnetron sputtering to fabricate FeCoNi medium-entropy alloy films. The effects of sputtering gas pressure and power on microstructure, surface morphology, and static/high-frequency magnetic properties were systematically investigated. In situ Lorentz transmission electron microscopy revealed the evolution patterns of magnetic domains. Findings indicate that low sputtering pressure (1 mTorr) promotes the formation of well-crystallised face-centred cubic (FCC) structures with dense, flat surfaces and superior soft magnetic properties. Conversely, high pressure induces amorphisation, increased surface roughness, and significant degradation of magnetic performance. Under optimised pressure conditions, a sputtering power of 100 W yielded the highest crystallinity and smoothest surface, demonstrating optimal static and high-frequency soft magnetic properties: high remanence ratio, low coercivity, and distinct ferroresonance behaviour across 2–7.5 GHz. FeCoNi films prepared under the optimal conditions (1 mTorr, 100 W) exhibited a nanocrystalline structure with uniform elemental distribution. In-situ magnetic domain observations revealed weak domain pinning effects, enabling consistent precession of magnetic moments during magnetisation—a phenomenon highly consistent with the high-frequency performance. This study establishes intrinsic correlations between process parameters, microstructure, magnetic properties, and domain dynamics, providing experimental evidence and theoretical guidance for the controlled fabrication of FeCoNi soft magnetic films and their application in high-frequency devices.

Author Contributions: X.Z. and Y.G. contributed equally to this work. Conceptualization, X.Z. and Y.G.; methodology, X.Z., Y.G. and Z.F.; writing—original draft preparation, X.Z., Y.G., Z.F. and K.C.; writing—review and editing, X.Z., Y.G., Z.F., K.C., G.J. and L.J.; visualization, X.Z. and Y.G.; project administration, L.J.; funding acquisition, L.J. All authors have read and agreed to the published version of the manuscript.

Funding: This research was funded by National Natural Science Foundation of China (12404250), the Natural Science Foundation of Zhejiang Province (LQN25A040008).

Institutional Review Board Statement: Not applicable.

Informed Consent Statement: Not applicable.

 doi:10.20944/preprints202603.0032.v1

Data Availability Statement: Data underlying the results presented in this paper are not publicly available at this time but may be obtained from the authors upon reasonable request.

Acknowledgments: The authors gratefully acknowledge the National Natural Science Foundation of China (12404250), the Natural Science Foundation of Zhejiang Province (LQN25A040008).

Conflicts of Interest: The authors declare no conflicts of interest.

References

1. J. M. Silveyra, E. Ferrara, D. L. Huber, T. C. Monson,Soft magnetic materials for a sustainable and electrified world Science 2018,362.
2. H. Lv, Z. Yang, B. Liu, G. Wu, Z. Lou, B. Fei, R. Wu,A flexible electromagnetic wave-electricity harvester Nat. Commun. 2021,12.
3. Y. Cai, J. Bai, H.-L. Shen, L. Huang, B. Rao, H. Wang,Development of Low-Cost Single-Chip Automotive 4D Millimeter-Wave Radar Sensors 2025,25.
4. M. Hollenbach, C. Kasper, D. Erb, L. Bischoff, G. Hlawacek, H. Kraus, W. Kada, T. Ohshima, M. Helm, S. Facsko, V. Dyakonov, G. V. Astakhov,Ultralong-Term High-Density Data Storage with Atomic Defects in SiC Adv. Funct. Mater. 2024,34.
5. M. Ghatge, G. Walters, T. Nishida, R. Tabrizian,An ultrathin integrated nanoelectromechanical transducer based on hafnium zirconium oxide Nature Electronics 2019,2: 506.
6. W. Yang, J. Liu, X. Yu, G. Wang, Z. Zheng, J. Guo, D. Chen, Z. Qiu, D. Zeng,The Preparation of High Saturation Magnetization and Low Coercivity Feco Soft Magnetic Thin Films via Controlling the Thickness and Deposition Temperature Materials 2022,15.
7. O. Acher, S. Dubourg,Generalization of Snoek's law to ferromagnetic films and composites Phys. Rev. B 2008,77.
8. L. J. Heyderman, M. Kläui, R. Schäublin, U. Rüdiger, C. A. F. Vaz, J. A. C. Bland, C. David,Fabrication of magnetic ring structures for Lorentz electron microscopy J. Magn. Magn. Mater. 2005,290-291: 86.
9. G. Herzer,Modern soft magnets: Amorphous and nanocrystalline materials Acta Mater. 2013,61: 718.
10. V. Shukla,Review of electromagnetic interference shielding materials fabricated by iron ingredients Nanoscale Advances 2019,1: 1640.
11. H. Kockar, O. Demirbas, H. Kuru, M. Alper,Differences observed in properties of ternary NiCoFe films electrodeposited at low and high pH J. Mater. Sci.:Mater. Electron. 2012,24: 1961.
12. G. Scheunert, O. Heinonen, R. Hardeman, A. Lapicki, M. Gubbins, R. M. Bowman,A review of high magnetic moment thin films for microscale and nanotechnology applications Appl. Phys. Rev. 2016,3.
13. I. Tabakovic, V. Venkatasamy,Preparation of metastable CoFeNi alloys with ultra-high magnetic saturation (Bs = 2.4–2.59 T) by reverse pulse electrodeposition J. Magn. Magn. Mater. 2018,452: 306.
14. S. Kunwar, J. Arout Chelvane, M. Manivel Raja,Structural, magnetic and Magnetic-Microstructural properties of sputtered FeCoNi thin films J. Magn. Magn. Mater. 2023,572.
15. M. Jiao, Z. Lei, Y. Wu, J. Du, X.-Y. Zhou, W. Li, X. Yuan, X. Liu, X. Zhu, S. Wang, H. Zhu, P. Cao, X. Liu, X. Zhang, H. Wang, S. Jiang, Z. Lu,Manipulating the ordered oxygen complexes to achieve high strength and ductility in medium-entropy alloys Nat. Commun. 2023,14.
16. Y. Zhang, T. T. Zuo, Z. Tang, M. C. Gao, K. A. Dahmen, P. K. Liaw, Z. P. Lu,Microstructures and properties of high-entropy alloys Progress in Materials Science 2014,61: 1.
17. Z. Li, F. Wang, C. Zhao, Y. Liao, M. Gao, H. Zhang,Microstructural evolution and enhanced magnetic properties of FeCoNiZrx medium entropy alloy films J. Alloys Compd. 2024,971.
18. Z. Cheng, Q. Zhao, M. Tao, J. Du, X. Huang, C. Liu,Preparation of FeCoNi medium entropy alloy from Fe3+–Co2+–Ni2+ solution system International Journal of Minerals, Metallurgy and Materials 2024,32: 92.
19. W. Peng, Y. Xia, H. Xu, X. Tan,Tuning Corrosion Resistance and AC Soft Magnetic Properties of Fe-Co-Ni-Al Medium-Entropy Alloy via Ni Content Entropy 2024,26.
20. A. Arab, M. R. Mardaneh, M. H. Yousefi,Investigation of magnetic properties of MnZn-substituted strontium ferrite nanopowders prepared via conventional ceramic technique followed by a high energy ball milling J. Magn. Magn. Mater. 2015,374: 80.

 doi:10.20944/preprints202603.0032.v1

21. Y. Zhang, M. Zhang, D. Li, T. Zuo, K. Zhou, M. C. Gao, B. Sun, T. Shen,Compositional Design of Soft Magnetic High Entropy Alloys by Minimizing Magnetostriction Coefficient in (Fe0.3Co0.5Ni0.2)100−x(Al1/3Si2/3)x System Metals 2019,9.
22. C. Toparli, B. Ebin, S. Gürmen,Synthesis, structural and magnetic characterization of soft magnetic nanocrystalline ternary FeNiCo particles J. Magn. Magn. Mater. 2017,423: 133.
23. X. Tan, J. Li, S. Zhang, H. Xu,Enhanced DC and AC Soft Magnetic Properties of Fe-Co-Ni-Al-Si High-Entropy Alloys via Texture and Iron Segregation Metals 2024,14.
24. D. Jiang, Z. Yuan, Z. Zhu, M. Yao,NiCoCrFeY High Entropy Alloy Nanopowders and Their Soft Magnetic Properties Materials 2024,17.
25. J. Kitagawa, D. Shintaku,Magnetic Properties of High-Entropy Alloy FeCoNiTi ACS Omega 2024,9: 37197.
26. N. I. Muhammad Nadzri, D. S. C. Halin, M. M. Al Bakri Abdullah, S. Joseph, M. A. A. Mohd Salleh, P. Vizureanu, D.-P. Burduhos-Nergis, A. V. Sandu,High-Entropy Alloy for Thin Film Application: A Review Coatings 2022,12.
27. C. Rodwihok, S. Choopun, P. Ruankham, A. Gardchareon, S. Phadungdhitidhada, D. Wongratanaphisan,UV sensing properties of ZnO nanowires/nanorods Applied Surface Science 2019,477: 159.
28. A. Kosari Mehr, A. Kosari Mehr,Magnetron sputtering issues concerning growth of magnetic films: a technical approach to background, solutions, and outlook Applied Physics A 2023,129.
29. Z. Ma, T. Wu, Q. Li, K. Sun, C. Wu, X. Jiang, Z. Yu, Z. Lan,Dynamic magnetization resonance enhancement of Co-based soft magnetic thin films induced by two-step oblique angle deposition J. Alloys Compd. 2025,1043.
30. Y. Khaydukov, G. McCafferty, A. Dobrynin, A. Devishvili, A. Vorobiev, P. Bencok, R. Fan, P. Steadman, K. McNeill, M. Ormston,Improved performance of polycrystalline antiferromagnet/ferromagnet stack by nitrogen-assisted deposition Appl. Phys. Lett. 2025,126.
31. M. Tkadletz, C. Hofer, C. Wüstefeld, N. Schalk, M. Motylenko, D. Rafaja, H. Holzschuh, W. Bürgin, B. Sartory, C. Mitterer, C. Czettl,Thermal stability of nanolamellar fcc-Ti1-xAlxN grown by chemical vapor deposition Acta Mater. 2019,174: 195.
32. C. Song, Z. Han, J. Zhou, X. Wang, L. Zhang, Z. Ma, L. Ma, F. Zheng,Regulation of static and dynamic magnetic properties of amorphous FeCoZr composition gradient films by Zr doping AIP Advances 2023,13.
33. Z. He, Z. Ma, Z. Li, Y. Du, J. Yang, C. Wu, Q. Li, X. Jiang, C. Wang, Z. Yu, Z. Lan, K. Sun,Strain Modulation of Microstructure, Magnetic Domains, and Magnetic Properties of Ti/Fe/Ni81Fe19/Fe/Ti Multilayer Thin Films Coatings 2023,13.
34. G. Vashisht, U. Shashank, S. Gupta, R. Medwal, C. L. Dong, C. L. Chen, K. Asokan, Y. Fukuma, S. Annapoorni,Pinning-assisted out-of-plane anisotropy in reverse stack FeCo/FePt intermetallic bilayers for controlled switching in spintronics J. Alloys Compd. 2021,877.
35. X. Fu, X. Wu, Q. Yu,Dislocation plasticity reigns in a traditional twinning-induced plasticity steel by in situ observation Materials Today Nano 2018,3: 48.
36. L. Ji, R. Zhao, X. Hu, C. Hu, X. Shen, X. Liu, X. Zhao, J. Zhang, W. Chen, X. Zhang,Reconfigurable Ferromagnetic Resonances by Engineering Inhomogeneous Magnetic Textures in Artificial Magnonic Crystals Adv. Funct. Mater. 2022,32.
37. X. Shen, L. Bo, R. Zhao, C. Hu, L. Ji, J. Zhang, X. Zhang, X. Dong,Spontaneous nucleation of vortex–antivortex pairs in confined magnetic microstructures J. Phys. D:Appl. Phys. 2023,57.